Published in final edited form as:
J Phys Chem B. 2013 December 12; 117(49): 15804–15811. doi:10.1021/jp407052a.

The pH-Dependent Picosecond Structural Dynamics in the Distal Pocket of Nitrophorin 4 Investigated by 2D IR Spectroscopy

Mark Cheng[⊥,┼], **Jennifer F. Brookes**[⊥,┼], **William R. Montfort**[‖], and **Munira Khalil**[⊥,*]

[⊥]Department of Chemistry, University of Washington, Seattle, Washington 98195

[‖]Department of Chemistry and Biochemistry, University of Arizona, Tucson, Arizona 85721

Abstract

Nitrophorin 4 (NP4) belongs to a family of pH-sensitive, nitric oxide (NO) transporter proteins which undergo a large structural change from a closed to an open conformation at high pH to allow for NO delivery. Measuring the pH-dependent structural dynamics in NP4–NO around the ligand binding site is crucial for developing a mechanistic understanding of NO binding and release. In this study we use coherent two-dimensional infrared (2D IR) spectroscopy to measure picosecond structural dynamics sampled by the nitrosyl stretch in NP4–NO as a function of pH at room temperature. Our results show that both the closed and open conformers of the protein are present at low (pD 5.1) and high (pD 7.9) pH conditions. The closed and open conformers are characterized by two frequencies of the nitrosyl stretching vibration labeled A_0 and A_1, respectively. Analysis of the 2D IR lineshapes reveals that at pD 5.1, the closed conformer experiences structural fluctuations arising from solvation dynamics on a ∼3 ps timescale. At pD 7.9, both the open and closed conformers exhibit fluctuations on a ∼1 ps timescale. At both pD conditions, the closed conformers maintain a static distribution of structures within the experimental time window of 100 ps. This is in contrast to the open conformer, which is able to interconvert among its sub-states on a ∼100 ps timescale. Our results directly measure the timescales of solvation dynamics in the distal pocket, the flexibility of the open conformation at high pH, and the rigidity of the closed conformers at both pH conditions. We discuss how the pH dependent equilibrium structural fluctuations of the nitrosyl ligand measured in this study are related to the uptake and delivery of nitric oxide in Nitrophorin 4.

Keywords

protein dynamics; heme proteins; nitrosyl stretching vibration; nitric oxide delivery; frequency-frequency correlation functions

I. Introduction

Nitrophorins (NPs) are a particular class of nitrosyl binding heme proteins found naturally in the saliva of blood feeding insects. In these proteins, NO is stored in the low pH environment of the salivary gland (pH ∼5) and is released in the higher pH environment of the host tissue (pH ∼7.5) to induce vasodilation and prevent blood coagulation.[1,2] Nitric oxide is a reactive messenger molecule implicated in regulating the immune, nervous and cardiovascular systems of mammals.[3] Given the importance of NO in biology, the NPs serve as excellent models to probe the interplay of structure, dynamics and function for a naturally occurring NO delivery system. Nitrophorin 4 is a widely studied protein of the Nitrophorin

*Corresponding Author: mkhalil@chem.washington.edu.
┼Author Contributions: These authors contributed equally.

family. Figure 1 shows a high-resolution crystal structure of the NP4-NO protein acquired at pH 5.6. The protein structure consists of an eight-stranded antiparallel β-barrel with a heme buried at one end. The protein is known to undergo a conformational change upon binding to NO, such that the A-B (residues 31-37) and the G-H (residues 125-132) loops pack tightly together to form a hydrophobic pocket preventing NO escape.[4-6] Crystal structures of NP4 reveal a distal pocket with structurally distinct closed and open conformations.[6] The closed conformation is characterized by a dynamic hydrophobic cavity with a network of hydrogen bonds between the residues of the A-B and G-H loops. The hydrogen bond network is disrupted in the open conformation resulting in a more hydrophilic cavity with the presence of water molecules and flexible loop regions. The two conformations are found to exist at all pH conditions by X-ray crystallography, with the fraction of the open conformation increasing at higher pH.[6]

Kinetic studies of the binding and dissociation of NO using histamine displacement and laser photolysis have revealed multi-exponential pH-dependent NO release rates across a wide range of timescales.[7-10] The pH dependence of the NO release is completely eliminated for the double mutant D129A/L130A confirming that the conformational flexibility of the loop regions is responsible for the pH-dependent NO release in NP4.[7] However, the cause for the non-exponential NO release rates remains an open question. There have been several molecular dynamics simulations on the NO release dynamics of NP4.[11-15] These simulations have revealed the importance of the flexibility of the loop regions, the protonation state of Asp 30 and the equilibrium of the closed and open conformers to the pH dependent NO release mechanism in the NP4 protein.

While the structural flexibility of the A-B and G-H loops and the polarity of the distal pocket have been extensively discussed in experimental and theoretical studies of NP4-NO, there have been no measurements of the timescales of equilibrium structural fluctuations of the nitrosyl ligand. The time-dependent frequency fluctuations ($\delta\omega(t)$) of an IR active vibration (ω_0) are encoded in the frequency-frequency correlation function (FFCF, $\langle\delta\omega(t)\delta\omega(0)\rangle$). Two-dimensional (2D) IR spectroscopy has been used effectively to measure the FFCF of carbonyl and nitrosyl ligands in heme proteins to characterize the structural fluctuations around the ligand binding sites.[16-24] There is a growing body of literature on how the frequency shifts of the nitrosyl stretching vibration (ν_{NO}) in heme proteins are a sensitive reporter of the local electric field and Fe-NO bonding interactions.[25-27]. The goal of this study is to measure the equilibrium structural dynamics in the distal pocket of NP4–NO as a function of pH using 2D IR spectroscopy to measure the FFCF of the ν_{NO}. Our experiments sample the conformational heterogeneity and directly measure the timescales of equilibrium structural fluctuations in the vicinity of the Fe–NO bond. We discuss how the spectroscopic data reveal a dynamic distal pocket environment that is crucial for the binding, release and regulation of NO in NP4.

II. Methods

Sample preparation

Nitrophorin 4 was overexpressed from an *Escherichia coli* strain and refolded from inclusion bodies supplemented with heme, as described previously.[4] In order to resolve the weak mid-IR absorption band of the NO stretching vibration at ∼1905 cm^{-1} from the absorbance of H_2O in the same spectral region, samples of purified ferric NP4 underwent a buffer exchange process to replace the 20 mM sodium phosphate buffer (at pH 7.0) with a deuterated buffer. Acidic (pD 5.1) and basic (pD 7.9) 20 mM potassium dideuterium phosphate (KD_2PO_4) buffer solutions were prepared in D_2O. Centrifugal filter devices (Amicon Ultra-0.5) were used to exchange the aqueous buffer as well as to concentrate the protein samples. In order to prepare the ferric NP4–NO complex, fresh NO gas was

generated by mixing ascorbic acid (880 mg in 25 mL of water) and sodium nitrite (40-60 mg) after degassing each of them under Ar for at least 30 minutes. The sample was also degassed for at least 15 minutes prior to flushing with the generated NO gas using an airtight syringe. Linear FTIR (Jasco FT/IR-4100) and UV-Vis (Jasco V-630) spectra of the samples were obtained (sample path length = 50 μm) before and after each 2D IR scan to ensure that the protein had not degraded during the experiment. The final concentrations of the protein sample at the start of each scan were determined by the intensity of the alpha and beta bands in the UV-Vis spectra of ferric NP4-NO.[28] The final concentrations were 6.4 mM and 4.1 mM for the acidic and basic samples, respectively. These concentrations yield an OD of 0.046 and 0.037 for the ν_{NO} peak at 1905 cm^{-1}.

2D IR Experiment

Femtosecond pulses of mid-IR light were generated from a combination of commercial equipment, beginning with a regenerative amplifier (Spectra Physics Spitfire Pro-35F-XP), which outputs 3 W, 800 nm, 35 fs pulses of light at 1 kHz. Approximately 1 W of the 800 nm output is sent to an optical parametric amplifier (OPA-800C) to produce the near-IR signal and idler pulses. The two near IR fields undergo difference frequency mixing in a 0.5 mm $AgGaS_2$ crystal to generate 80 fs mid-IR pulses with a spectral bandwidth of ∼200 cm^{-1} at a center wavelength of 5.1 μm.

The mid-IR pulse is sent into a five-beam interferometer to generate three input pulses, a tracer beam and a local oscillator field as described previously.[29,30] The three input IR beams have parallel polarizations and are arranged in a “boxcar” geometry, temporally overlapped, and focused onto the sample with a spot-size of ∼150 μm. Each of the input beams has 0.2 μJ of energy per pulse. The home-built sample cell is equipped with two 1 mm CaF_2 windows and a 50 μm Teflon spacer. The resulting background-free signal field is overlapped with the local oscillator field on a beamsplitter for heterodyne detection. The reflected and transmitted combined signal and local oscillator fields are π out of phase with respect to each other and are detected at the focal plane of a spectrometer (Triax 190, Horiba Jobin Yvon, 150 1ines/mm grating) using a 2 × 64 mercury cadmium telluride (MCT) array detector (IR0144, Infrared Systems Development). We subtract signals from the two linear MCT arrays to perform “balanced detection” on a shot-to-shot basis as explained in Ref 30.

The evolution (τ_1) and waiting (τ_2) time delays between the consecutive pairs of pulses 1,2 and 2,3 are accurately controlled by Newport XMS50 linear stages. Rephasing and non-rephasing experiments were performed at each τ_2 delay in order to construct absorptive 2D IR correlation spectra. The τ_1 delay was scanned in 4 fs steps from 0 to 4(3) ps for the rephasing (non-rephasing) experiments. The τ_2 delay was scanned in unequal time steps from 0 to 70 ps in unequal time steps with each data point representing 2000 laser shots. The raw experimental data was zero padded to 32.8 ps and Fourier transformed along τ_1 to obtain the ω_1 axis. The final 2D IR spectrum is corrected for the phase ambiguities corresponding to drift of the relative timing between the local oscillator and signal fields by comparing the projection of the 2D IR spectrum along the ω_1 axis to a two-beam dispersed pump-probe spectrum collected for the same values of τ_2.[31]

2D IR spectral fitting

The experimental 2D IR spectra were fit by iteratively calculating the third-order nonlinear signal field as a function of τ_1 and τ_3 in the time domain and then Fourier transforming it to obtain theoretical spectra as described previously.[29] 2D IR spectra of NP4 under both pH conditions were simulated using a six-level system for two non-interacting NP4-NO populations, each with a ground, first-excited and second-excited vibrational state (0, 1, 2) using the nonlinear response formalism detailed previously.[32,33] In our system, there are a

total of 12 response functions for the rephasing and non-rephasing signals. We ignore any cross correlation terms between the two non-interacting NP4-NO populations since the experiment does not reveal the presence of any cross-peaks. We assume a separation of timescales for the vibrational and rotational dynamics for calculating the third-order nonlinear response functions.

The goal of the spectral fitting procedure is to extract parameters of the FFCF of the ν_{NO} in NP4-NO as a function of pH. We modeled the 2D lineshapes using the following form for the FFCF:

$$C_{11}(t)=\sum_{n=1}^{2}\Delta_n^2\exp\left(-\frac{t}{\tau_{cn}}\right)+\frac{\delta(t)}{T_2^*} \quad (1)$$

In the above expression, Δ_n and τ_{cn} describe the amplitude and timescales of the frequency fluctuations in the Kubo model, $\delta(t)$ is the Dirac delta function and T_2^* represents the timescales of fast dynamics determining the homogenous linewidth of the ν_{NO} in NP4-NO. Analytical expressions for the nonlinear dephasing functions in terms of the correlation functions are obtained using the methodology described in Ref. 33. The contribution of the rotational correlation functions to the 2D IR lineshape was not included because of the long time scales associated with orientational rearrangement of the protein. We accounted for the effects of vibrational population relaxation by introducing exponential relaxation rates into the vibrational response functions during all three time periods using harmonic scaling rules. For example, if the vibrational lifetime for the first excited state of ν_{NO} is T_1, then the vibrational lifetime of the second excited state is $1/2T_1$. The vibrational lifetime of the first excited state of ν_{NO} for both the sub-populations of NP4-NO was determined to be 30 ps using IR pump-probe experiments. Harmonic scaling was used for the energy gap fluctuations in our two separate 3-level systems to relate the FFCFs of the first (1) and second (2) vibrational states of our three level system, such that: $C_{\mathbf{22}}(t) = 2C_{\mathbf{21}}(t) = 2C_{\mathbf{12}}(t) = 4C_{\mathbf{11}}(t)$. For each pH condition, the experimental 2D IR spectra for all τ_2 points were fit simultaneously by floating the parameters in the FFCFs, the vibrational anharmonicity ($\Delta_{12}=2\nu_{NO}^{1\leftarrow0}-\nu_{NO}^{2\leftarrow0}$), and the transition dipole moment between the first and second excited states($|\mu_{\mathbf{12}}|$) for each of the sub-populations of NP4-NO. The best-fit values are listed in Table 2. The simulated and experimental spectra were fit using a nonlinear least squares fitting routine written in MATLAB.

III. Results and Discussion

A. pH-Dependent FTIR Spectra and conformational sub-states of NP4-NO

The FTIR spectrum of NP4–NO in the ν_{NO} region is shown in Figure 2 as a function of pH. The spectra show two peaks in the ν_{NO} region centered at ~1905 and ~1917 cm^{-1}. We see that the peak at 1917 cm^{-1} increases in amplitude under higher pH conditions. The shaded areas represent fits to the two peaks using Voigt lineshapes and the best-fit parameters are listed in Table 1. The two peaks in the ν_{NO} region indicate the presence of two conformational sub-states of the NP4-NO protein which exist under acidic and basic pH conditions. Previous FTIR and Raman studies of NP4-NO have assigned the peak centered at ~1905 cm^{-1} to the closed conformation where the NO ligand is in a hydrophobic environment and the peak at ~1917 cm^{-1} to the open conformation with a hydrophilic distal pocket.[8,25,34] The shift of the ν_{NO} vibration to higher frequencies in more hydrophilic/polar environments is also seen in other Fe–NO complexes like sodium nitroprusside.[29,35] In this work, we label the peak at ~1905 cm^{-1} as A_0 and the peak at ~1917 cm^{-1} as A_1. The

labeling scheme follows from the FTIR spectroscopy of ferric myoglobin-NO ($Mb^{III}NO$) under various pH conditions.[36,37]

High-resolution crystal structures of NP4-NO at pH 5.6 and 7.5 have revealed the presence of at least two major conformers and considerable loop disorder at higher pH.[6] Figures 3(a-b) display the distal pocket configuration for the closed and open conformational sub-states of NP4-NO at pH 5.6. We see that in the closed conformation the hydrogen bonding interaction between the residues of the A-B and G-H loops is preserved, the non-polar residues are packed into the binding pocket providing favorable non-polar interactions with the NO ligand. In contrast, the open conformation shows that Leu 130 has moved away from the distal pocket, providing room for several solvent molecules. The position of the electron density of Leu 130 in the open conformer matches closely with the NP4-NH_3 crystal structure at pH 7.4, which shows the presence of several (∼5) water molecules in the distal pocket.[6] In the refined crystal structure of NP4-NO at pH 5.6, the open conformer was found to have an occupancy of 0.29. Based on the crystal structures and the pH-dependent FTIR spectra, we assign the A_0 and A_1 peaks in Figure 2a to the closed and open conformational sub-states of NP4-NO at pH 5.6.

The closed and open conformers of the high resolution crystal structure of NP4-NO at pH 7.5 are shown in Figures 3c-d. The x-ray study has noted the difficulty in modeling loops A-B and G-H because of considerable disorder. The structural distinction between the closed and open conformers is seen in the residues 129-131. Leucine 130 flips its position between the closed and open conformational sub-states in a manner similar to the crystal structure obtained at pH 5.6. Water molecules are seen in the distal pocket within ∼3.8 Å of the nitrosyl ligand in the crystal structure at higher pH. Given that the frequencies of the ν_{NO} peaks are very similar at both pH conditions, we assign the A_0 and A_1 peaks in Figure 2b to the closed and open conformational sub-states of NP4-NO at pH 7.5.

The ν_{NO} peak assignments described above agree with the studies on ferric Mb-NO and DFT calculations.[25,36,37] In wild type $Mb^{III}NO$ at room temperature, a major peak at ∼1927 cm^{-1} and a weak feature at ∼1902 cm^{-1} are observed in the ν_{NO} region at neutral pH.[38] The mutant, H64L, of $Mb^{III}NO$ shows a single peak at 1904 cm^{-1}. The negative polar interaction of the nitrosyl ligand with a tautomeric form of the distal histidine has been proposed for the protein conformer giving rise to the peak at 1927 cm^{-1} in wild type $Mb^{III}NO$.[37] The absence of this interaction in the H64L mutant, results in the downshift of the ν_{NO} frequency to 1904 cm^{-1}, which is very similar to the frequency of the A_0 peak in NP4-NO. The DFT calculations have shown how the frequency of the ν_{NO} in ferric heme proteins reports on the polarity of the heme protein and interactions of the NO moiety with nearby Lewis base donors.[25] The same DFT study has assigned an increase in frequency of the ν_{NO} in open conformer of NP4-NO to lone pair interactions of the NO with a water molecule.

The fits of peaks in the ν_{NO} region reveal that the fraction of the A_1 peak is 16% and 26% at pD 5.1 and 7.9 respectively. Previous FTIR studies of NP4-NO had measured a ratio of 0.2 at cryogenic temperatures for NP4-NO at pH 7.5.[8] The linewidths of the peaks in the FTIR spectra range from 12-14 cm^{-1} and are governed by the frequency-frequency correlation function (FFCF) of the ν_{NO} vibration, which measures the timescales of structural dynamics around the NO binding site for the open and closed conformations. Using 2D IR lineshape analysis we can measure the timescales of frequency fluctuations, which dictate the linewidth of the ν_{NO} in NP4-NO as a function of pH.

B. pH-dependent 2D IR spectra and extraction of the FFCF parameters

The top panel of Figure 4 displays a series of experimental 2D IR spectra of the ν_{NO} in NP4–NO plotted as a function of τ_2 at pD 5.1. In each of the spectra, the positive diagonal

peaks correspond to vibrational transitions between the ground and first excited state of the $\nu_{NO}(\nu_{NO}^{0\rightarrow1})$. The off-diagonal negative peaks involve transitions between the first and second excited states of the $\nu_{NO}(\nu_{NO}^{1\rightarrow2})$. The separation of the two peaks in the ω_3 dimension of the 2D IR plots is a direct measure of the vibrational anharmonicity of the ν_{NO} in NP4–NO. Focusing on the strong positive 2D peaks in Figure 4a, we note that they are elongated along the diagonal axes at τ_2=0.2 ps representing a distribution of structures for the closed (A_0) and open (A_1) conformations of NP4-NO at low pH. As τ_2 increases, structural fluctuations cause the vibrational frequencies to lose correlation and results in the 2D lineshapes becoming more symmetric. It is important to note that the A_0 peak remains elongated along the diagonal even at τ_2 = 70 ps. A qualitative comparison between the A_0 and A_1 peaks at τ_2 = 70 ps suggests that the latter peak undergoes faster frequency fluctuations. The evolving 2D lineshape is a direct measure of the FFCF and provides information on the amplitude and timescales of the structural fluctuations in the open and closed conformations of NP4–NO.

We fit the 2D IR spectra to extract the parameters of the FFCF as described in the Methods section. In this paper we focus our efforts on understanding the 2D IR lineshape of the fundamental transition of the ν_{NO} in NP4–NO. The bottom panel in Figure 4 displays the 2D IR spectra resulting from the best fits of the experimental spectra assuming the form of the correlation functions given by Equation 1. The resulting parameters of the FFCF are listed in Table 2. We find that the homogenous dephasing time (T_2^*) for the A_0 and A_1 peaks of the ν_{NO} in NP4-NO at pD 5.1 is 7 ps. While the homogenous contribution to the spectral linewidth is similar for the A_0 and A_1 peaks, the timescales for structural diffusion (τ_{c1} and τ_{c2}) are very different. The ν_{NO} of the closed conformer exhibits fast structural fluctuations on a 3 ps timescale (τ_{c1}). Significant portions of the dynamics are too slow to be measured on our experimental timescale of ~100 ps. This is represented as $\tau_{c2}=\infty$ in Table 2. The ν_{NO} of the open conformer exhibits structural fluctuations on a 0.9 ps and a 130 ps timescale. The ratio of the amplitudes of the structural fluctuations (Δ_2/Δ_1) is 1 and 3.5 for the A_0 and A_1 peaks.

Figure 5 shows the experimental and best fit 2D IR spectra for the ν_{NO} in NP4-NO obtained at pD 7.9. At τ_2=0.2 ps, the A_0 and A_1 peaks are elongated along the diagonal indicating the presence of structural inhomogeneity in the two conformational sub-states. Similar to the 2D IR data taken at pD 5.1, the A_1 peak loses its frequency correlation faster than the A_0 peak as evidenced by their different 2D lineshapes at τ_2=25 ps. Our best fits to the 2D IR data (see Table 2) find that the vibrational anharmonicity is pH independent and is ~30 cm^{-1} for peaks A_0 and A_1 peaks. The ν_{NO} of the closed conformer exhibits fast structural fluctuations on a 1.4 ps timescale (τ_{c1}) and on timescales longer than our experimental time window of ~100 ps. This is represented as $\tau_{c2}=\infty$ in Table 2. The ν_{NO} of the open conformer exhibits structural fluctuations on a 0.8 ps and a 70 ps timescale. The ratio of the amplitudes of the structural fluctuations (Δ_2/Δ_1) is 1 and 2 for the A_0 and A_1 peaks.

The homogenous contribution to the IR linewidth is governed by protein and solvent fluctuations much faster than the experimental time window of a 2D IR experiment. The measured homogenous timescale (T_2^*), falls within the range of 5–12 ps for the ν_{CO} in myoglobin-CO, neuroglobin-CO and for cyt-$P450_{cam}$-CO substrate complexes.[16,20] In particular, the homogenous dephasing time for the H64V mutant of myoglobin-CO was measured to be 7.7 ps. In contrast, the homogenous dephasing time for the ν_{NO} of sodium nitroprusside ($Na_2Fe(CN)_5NO{\cdot}2H_2O$, SNP) dissolved in various polar solvents was measured to be ~2 ps.[29,39] These comparisons suggest that the dephasing timescales are slower in non-polar environments such as the distal pocket of NP4-NO in contrast to the polar solvent environments experienced by the ν_{NO} of sodium nitroprusside. The vibrational

anharmonicity value of ~29.5 cm^{-1} for the A_0 and A_1 peaks extracted from the fits of the 2D IR spectra is not affected by pH. This value is similar to the measured anharmonicity of 29 cm^{-1} for the ν_{NO} in wild-type Mb^{III} NO and 28 cm^{-1} for the ν_{NO} in ferric cytochrome C-NO.[24]

The closed conformer at acidic pH is characterized by a well packed distal pocket where the NO is surrounded by non-polar residues held together by hydrogen bonding interaction between the A-B and G-H loops as seen in Figure 3a. In contrast, the open conformation at the acidic pH is characterized by greater disorder in the A-B and G-H loops and displays room for several water molecules in the distal pocket.[6] The FFCF of the A_0 and A_1 peaks exhibits spectral diffusion on 3 and 1.4 ps timescales, respectively. The crystal structures of the distal pocket at a higher pH are characterized by a greater degree of loop flexibility and the presence of several water molecules near the nitrosyl binding site. The FFCF of the A_0 and A_1 peaks in the pD 7.9 sample exhibits spectral diffusion on a 1.4 and 0.8 ps timescales, respectively. We assign the fast timescales to fluctuations of the local electric field around the nitrosyl ligand in NP4-NO for the closed and open protein conformers. Our previous work on characterization of the FFCF of the ν_{NO} in SNP found a negative correlation between the solvent polarity and the timescale for spectral diffusion.[29] The solvent polarity was defined by the empirical solvent parameters: $E_T^N(30)$ and the acceptor number (AN).[40] It is interesting to note that the τ_{c1} timescale of the ν_{NO} in NP4-NO mentioned above are very similar to the measured τ_{c1} values of ν_{NO} in SNP dissolved in ethanol (3.2 ps), methanol (2.3 ps), D_2O (1.4 ps) and H_2O (0.84 ps). Based on the above comparison, we propose that the polarity of the protein distal pocket in the closed and open conformers at pD 5.1 can be characterized by a maximum $E_T^N(30)$ value corresponding to that of ethanol $(E_T^N(30)=0.65)$ and water $(E_T^N(30)=1)$, respectively. The timescale for spectral diffusion of the closed conformer changes from 3 to 1.4 ps on increasing the sample pH. This can be explained by the presence of water molecules reported in the crystal structure resulting in an increase in the polarity of the distal pocket upon increasing the sample pH.

The 2D IR lineshape study also reveals the presence of slow (τ_{c2}) frequency fluctuations of the closed and open conformers. The frequency fluctuations of the ν_{NO} in the closed conformer under all pH conditions are too slow to be measured on the timescale of our experiment and appear static. In contrast the ν_{NO} in the open conformer undergoes frequency fluctuations on the 130 ps and 70 ps timescale for the pD 5.1 and 7.9 samples respectively. We attribute these long timescale dynamics to the structural dynamics of the loop regions of NP4-NO. These dynamics appear to be frozen for the closed conformers on the 100 ps timescale. However, the loop dynamics are faster for the open conformers. Our finding is consistent with X-ray crystallography studies, where it has been found that the A-B and G-H loops are poorly modeled for the open conformers of the NP4-NO protein.[6]

The carbonyl ligand has been used extensively as a vibrational probe in 2D IR studies to measure structural dynamics in the active site of several heme proteins.[16-22] These studies have measured timescales for spectral diffusion on 1-10 ps timescales and also slower timescales ranging from 60-300 ps. The fast timescales can be characterized as local structural fluctuations around the CO probe and the slower fluctuations have been attributed to global motions involving the entire protein. For example, molecular dynamics simulations have demonstrated that the experimentally measured timescales in the FFCF of the ν_{CO} in wild type and mutant myoglobin-CO are governed by the dynamics of the distal histadine ligand, and protein-water interactions.[18,22,41,42] 2D IR studies of the ν_{NO} in wild-type $Mb^{III}NO$ and ferric cytochrome C-NO have measured vibrational frequency fluctuation timescales of 3.3 ps and 5.2 ps, respectively.[23,24] The ν_{NO} in the H64Q-NO mutant of $Mb^{III}NO$ exhibits a slower timescale of ~10 ps in the measured FFCF.[24] A reduction in

polar interactions with the nitrosyl ligand in the mutant without the distal histidine, results an increase in the timescale of frequency fluctuations which is in keeping with the trend seen in NP4-NO.

C. Relating structure, function and dynamics in Nitrophorin 4

The results and discussion of the 2D IR lineshape analysis reveals a picture of a dynamic distal pocket with structural fluctuations on a range of timescales. We next discuss how our measurement of the equilibrium structural fluctuations in the distal pocket of the open and closed conformers of NP4–NO at two different pH conditions shed light on the function of this NO transporter protein. The binding and release of NO from the heme has been described as the following two step process:[7]

$$\mathrm{NP\text{-}\ NO} \underset{k_{on}}{\overset{k_{off1}/k_{off2}(\mathrm{pH\ \ dep.})}{\rightleftarrows}} [\mathrm{NP:\ NO}] \underset{k_{-1}}{\overset{k_1}{\rightleftarrows}} \mathrm{NP{+}NO}$$

In this model, NO dissociation occurs with two pH-dependent rates ($k_{off1,2}$) involving a slow protein conformational change of the protein and a faster rate (k_1) representing release from the open conformation. It has been shown that the pH dependence of the slower off-rates can be attributed to the flexibility and dynamics of the loop regions from various mutant studies which have destabilized the closed conformation and altered the pH dependence of the equilibrium populations of the open and closed conformers.[7,10] Ultrafast rebinding studies following photodissociation of NO from ferric NP4-NO have measured a 10-25 ps and a >150 ps timescale for geminate recombination.[9] The faster timescale has been attributed to NO rebinding from a hydrophobic closed conformer and the longer timescale has been attributed to rebinding from the hydrophilic open conformer.

Our results demonstrate that there is a static distribution of the closed conformers at both pH conditions and a distribution of interconverting open conformers on the ∼100 ps timescale. These heterogeneous structures arising from different interactions of the NO and its local environment in the distal pocket, would allow for slightly different rates of thermal bond cleavage resulting in a truly non-exponential ligand release process. The results in this study provide experimental verification for MD simulations which have suggested that the structural loops in NP4 should not be viewed as rigid cages that confine NO, but rather as a “dynamical oil droplet” that contains NO within the fluctuating nonpolar pocket.[6,11] We directly measure timescales of 3 ps and ∼1 ps for fast structural fluctuations in a hydrophobic and hydrophilic environment of the distal pocket.

We plan to perform 2D IR studies on mutants of NP4 where several key residues in the A-B and G-H loops have been replaced to affect the binding and release rates of NO, in the future. Measuring the FFCF of the ν_{NO} in these mutants will allow us to directly probe the correlation between equilibrium structural fluctuations in the distal cavity and the function of this NO transporter protein. The rates of NO binding/release to ferric myoglobin are 10/2000 fold faster than those for NP4, in addition to being described by a single phase.[43] A recent study has measured the FFCF of the ν_{NO} in wild-type $Mb^{III}NO$ to have a timescale of 3 ps and significant portions of the dynamics were too slow to measure on the experimental timescale.[24] In comparison with the NP4-NO 2D IR results presented in this manuscript, the ν_{NO} in wild-type $Mb^{III}NO$ lacks equilibrium structural fluctuations on the 70-100 ps timescale. This suggests that the equilibrium frequency fluctuations arising from local electric field fluctuations in the distal pocket and the loop dynamics have a role to play in regulating the uptake and diffusion of the nitrosyl ligand in NP4.

IV. Summary

In summary, we use 2D IR spectroscopy to measure the picosecond structural dynamics in the distal pocket of NP4–NO. We assign the A_0 and A_1 peaks in the nitrosyl stretching region of the FTIR to the ν_{NO} of the closed and open conformers of NP4-NO present at pD 5.1 and 7.9. The assignment is in agreement with previous IR and Raman studies of NP4-NO and $Mb^{III}NO$ and DFT calculations. The measured timescales of the FFCF for the A_0 and A_1 peaks are a quantitative description of the structural heterogeneity and solvent dynamics in the vicinity of the heme. The ability of the open conformer to exchange among its sub-states in ∼100 ps measures the structural flexibility of the loop regions. The spectroscopic data provides a microscopic explanation for the previously observed kinetic heterogeneity in the release rates of NO from the protein at all pH conditions. This study highlights how picosecond structural dynamics in the distal pocket of NP4-NO are linked to its function and could hold implications for ligand binding and release in other NO transport and receptor proteins.

Acknowledgments

We are grateful to Jacquie Brailey for protein preparation and to Madhumitha Balasubramanian for help with Figure 3. This work was supported by the NSF (CHE 0847790 to M.K.) and the NIH (HL062969 to W.R.M.). M.K. acknowledges additional support from the David and Lucille Packard Fellowship for Science and Engineering and the Alfred P. Sloan Foundation.

References

1. Walker FA, Montfort WR. The Nitric Oxide-Releasing Heme Proteins from the Saliva of the Blood-Sucking Insect Rhodnius Prolixus. Adv Inorg Chem. 2001; 51:295–358.
2. Ribeiro J, Hazzard J, Nussenzveig R, Champagne D, Walker F. Reversible Binding of Nitric Oxide by a Salivary Heme Protein from a Bloodsucking Insect. Science. 1993; 260:539–541. [PubMed: 8386393]
3. Bredt DS, Snyder SH. Nitric Oxide: A Physiologic Messenger Molecule. Ann Rev Biochem. 1994; 63:175–195. [PubMed: 7526779]
4. Andersen JF, Weichsel A, Balfour CA, Champagne DE, Montfort WR. The Crystal Structure of Nitrophorin 4 at 1.5 .Ang. Resolution: Transport of Nitric Oxide by a Lipocalin-Based Heme Protein. Structure (London). 1998; 6:1315–1327.
5. Weichsel A, Andersen JF, Roberts SA, Montfort WR. Nitric Oxide Binding to Nitrophorin 4 Induces Complete Distal Pocket Burial. Nat Struct Biol. 2000; 7:551–554. [PubMed: 10876239]
6. Kondrashov DA, Roberts SA, Weichsel A, Montfort WR. Protein Functional Cycle Viewed at Atomic Resolution: Conformational Change and Mobility in Nitrophorin 4 as a Function of pH and NO Binding. Biochemistry. 2004; 43:13637–13647. [PubMed: 15504026]
7. Maes EM, Weichsel A, Andersen JF, Shepley D, Montfort WR. Role of Binding Site Loops in Controlling Nitric Oxide Release: Structure and Kinetics of Mutant Forms of Nitrophorin 4. Biochemistry. 2004; 43:6679–6690. [PubMed: 15157102]
8. Nienhaus K, Maes EM, Weichsel A, Montfort WR, Nienhaus GU. Structural Dynamics Controls Nitric Oxide Affinity in Nitrophorin 4. J Biol Chem. 2004; 279:39401–39407. [PubMed: 15258143]
9. Benabbas A, Ye X, Kubo M, Zhang Z, Maes EM, Montfort WR, Champion PM. Ultrafast Dynamics of Diatomic Ligand Binding to Nitrophorin 4. J Am Chem Soc. 2010; 132:2811–2820. [PubMed: 20121274]
10. Abbruzzetti S, He C, Ogata H, Bruno S, Viappiani C, Knipp M. Heterogeneous Kinetics of the Carbon Monoxide Association and Dissociation Reaction to Nitrophorin 4 and 7 Coincide with Structural Heterogeneity of the Gate-Loop. J Am Chem Soc. 2012; 134:9986–9998. [PubMed: 22594621]

11. Swails JM, Meng Y, Walker FA, Marti MA, Estrin DA, Roitberg AE. Ph-Dependent Mechanism of Nitric Oxide Release in Nitrophorins 2 and 4. J Phys Chem B. 2009; 113:1192–1201. [PubMed: 19159340]
12. Marti MA, Estrin DA, Roitberg AE. Molecular Basis for the Ph Dependent Structural Transition of Nitrophorin 4. J Phys Chem B. 2009; 113:2135–2142. [PubMed: 19170552]
13. Marti MA, Gonzalez Lebrero MC, Roitberg AE, Estrin DA. Bond or Cage Effect: How Nitrophorins Transport and Release Nitric Oxide. J Am Chem Soc. 2008; 130:1611–1618. [PubMed: 18189390]
14. Kondrashov DA, Montfort WR. Nonequilibrium Dynamics Simulations of Nitric Oxide Release: Comparative Study of Nitrophorin and Myoglobin. J Phys Chem B. 2007; 111:9244–9252. [PubMed: 17622170]
15. Menyhard DK, Keseru GM. Protonation State of Asp30 Exerts Crucial Influence over Surface Loop Rearrangements Responsible for No Release in Nitrophorin 4. FEBS letters. 2005; 579:5392–5398. [PubMed: 16198351]
16. Thielges MC, Chung JK, Fayer MD. Protein Dynamics in Cytochrome P450 Molecular Recognition and Substrate Specificity Using 2d Ir Vibrational Echo Spectroscopy. J Am Chem Soc. 2011; 133:3995–4004. [PubMed: 21348488]
17. Bagchi S, Thorpe DG, Thorpe IF, Voth GA, Fayer MD. Conformational Switching between Protein Substates Studied with 2d Ir Vibrational Echo Spectroscopy and Molecular Dynamics Simulations. J Phys Chem B. 2010; 114:17187–17193. [PubMed: 21128650]
18. Bagchi S, Nebgen BT, Loring RF, Fayer MD. Dynamics of a Myoglobin Mutant Enzyme: 2d Ir Vibrational Echo Experiments and Simulations. J Am Chem Soc. 2010; 132:18367–18376. [PubMed: 21142083]
19. Ishikawa H, Kim S, Kwak K, Wakasugi K, Fayer MD. Disulfide Bond Influence on Protein Structural Dynamics Probed with 2d-Ir Vibrational Echo Spectroscopy. Proc Natl Acad Sci U S A. 2007; 104:19309–19314. [PubMed: 18042705]
20. Ishikawa H, Finkelstein IJ, Kim S, Kwak K, Chung JK, Wakasugi K, Massari AM, Fayer MD. Neuroglobin Dynamics Observed with Ultrafast 2d-Ir Vibrational Echo Spectroscopy. Proc Natl Acad Sci U S A. 2007; 104:16116–16121. [PubMed: 17916624]
21. Finkelstein IJ, Ishikawa H, Kim S, Massari AM, Fayer MD. Substrate Binding and Protein Conformational Dynamics Measured by 2d-Ir Vibrational Echo Spectroscopy. Proc Natl Acad Sci U S A. 2007; 104:2637–2642. [PubMed: 17296942]
22. Merchant KA, Noid WG, Akiyama R, Finkelstein IJ, Goun A, McClain BL, Loring RF, Fayer MD. Myoglobin-Co Substate Structures and Dynamics: Multidimensional Vibrational Echoes and Molecular Dynamics Simulations. J Am Chem Soc. 2003; 125:13804–11381. [PubMed: 14599220]
23. Hunt NT, Greetham GM, Towrie M, Parker AW, Tucker NP. Relationship between Protein Structural Fluctuations and Rebinding Dynamics in Ferric Haem Nitrosyls. Biochem J. 2011; 433:459–468. [PubMed: 21067516]
24. Adamczyk K, Candelaresi M, Kania R, Robb K, Bellota-Anton C, Greetham GM, Pollard MR, Towrie M, Parker AW, Hoskisson PA, et al. The Effect of Point Mutation on the Equilibrium Structural Fluctuations of Ferric Myoglobin. Phys Chem Chem Phys. 2012; 14:7411–7419. [PubMed: 22526234]
25. Soldatova AV, Ibrahim M, Olson JS, Czernuszewicz RS, Spiro TG. New Light on No Bonding in Fe(Iii) Heme Proteins from Resonance Raman Spectroscopy and Dft Modeling. J Am Chem Soc. 2010; 132:4614–4625. [PubMed: 20218710]
26. Spiro TG, Soldatova AV, Balakrishnan G. Co, No and O2 as Vibrational Probes of Heme Protein Interactions. Coord Chem Rev. 2013; 257:511–527. [PubMed: 23471138]
27. Park ES, Thomas MR, Boxer SG. Vibrational Stark Spectroscopy of No Bound to Heme: Effects of Protein Electrostatic Fields on the No Stretch Frequency. J Am Chem Soc. 2000; 122:12297–12303.
28. Maes EM, Roberts SA, Weichsel A, Montfort WR. Ultrahigh Resolution Structures of Nitrophorin 4: Heme Distortion in Ferrous Co and No Complexes. Biochemistry. 2005; 44:12690–12699. [PubMed: 16171383]

29. Brookes JF, Slenkamp KM, Lynch MS, Khalil M. Effect of Solvent Polarity on the Vibrational Dephasing Dynamics of the Nitrosyl Stretch in an Fe Complex Revealed by 2D IR Spectroscopy. J Phys Chem A. 2013 ASAP.
30. Lynch MS, Slenkamp KM, Cheng M, Khalil M. Coherent Fifth-Order Visible–Infrared Spectroscopies: Ultrafast Nonequilibrium Vibrational Dynamics in Solution. J Phys Chem A. 2012; 116:7023–7032. [PubMed: 22642262]
31. Khalil M, Demirdöven N, Tokmakoff A. Coherent 2D IR Spectroscopy: Molecular Structure and Dynamics in Solution. J Phys Chem A. 2003; 107:5258–5279.
32. Mukamel, S. Principles of Nonlinear Optical Spectroscopy. Oxford University Press; New York: 1995.
33. Sung J, Silbey RJ. Four Wave Mixing Spectroscopy for a Multilevel System. J Chem Phys. 2001; 115:9266.
34. Ding XD, Weichsel A, Andersen JF, Shokhireva TK, Balfour C, Pierik AJ, Averill BA, Montfort WR, Walker FA. Nitric Oxide Binding to the Ferri- and Ferroheme States of Nitrophorin 1, a Reversible No-Binding Heme Protein from the Saliva of the Blood-Sucking Insect, Rhodnius Prolixus. J Am Chem Soc. 1999; 121:128–138.
35. Sando GM, Zhong Q, Owrutsky JC. Vibrational and Rotational Dynamics of Cyanoferrates in Solution. J Chem Phys. 2004; 121:2158–2168. [PubMed: 15260770]
36. Nienhaus K, Palladino P, Nienhaus GU. Structural Dynamics of Myoglobin: FTIR-TDS Study of NO Migration and Binding. Biochemistry. 2007; 47:935–948. [PubMed: 18161992]
37. Miller LM, Pedraza AJ, Chance MR. Identification of Conformational Substates Involved in Nitric Oxide Binding to Ferric and Ferrous Myoglobin through Difference Fourier Transform Infrared Spectroscopy (FTIR). Biochemistry. 1997; 36:12199–12207. [PubMed: 9315857]
38. Park J, Lee T, Park J, Lim M. Photoexcitation Dynamics of No-Bound Ferric Myoglobin Investigated by Femtosecond Vibrational Spectroscopy. J Phys Chem B. 2013; 117:2850–2863. [PubMed: 23432208]
39. Tayama J, Ohta K, Tominaga K. Vibrational Transition Frequency Fluctuation of the No Stretching Mode of Sodium Nitroprusside in Aqueous Solutions. Chem Lett. 2012; 41:366–368.
40. Reichardt C. Solvatochromic Dyes as Solvent Polarity Indicators. Chem Rev. 1994; 94:2319–2358.
41. Massari AM, Finkelstein IJ, McClain BL, Goj A, Wen X, Bren KL, Loring RF, Fayer MD. The Influence of Aqueous Versus Glassy Solvents on Protein Dynamics: Vibrational Echo Experiments and Molecular Dynamics Simulations. J Am Chem Soc. 2005; 127:14279–14289. [PubMed: 16218622]
42. Williams RB, Loring RF, Fayer MD. Vibrational Dephasing of Carbonmonoxy Myoglobin. J Phys Chem B. 2001; 105:4068–4071.
43. Sharma VS, Traylor TG, Gardiner R, Mizukami H. Reaction of Nitric Oxide with Heme Proteins and Model Compounds of Hemoglobin. Biochemistry. 1987; 26:3837–3843. [PubMed: 3651417]

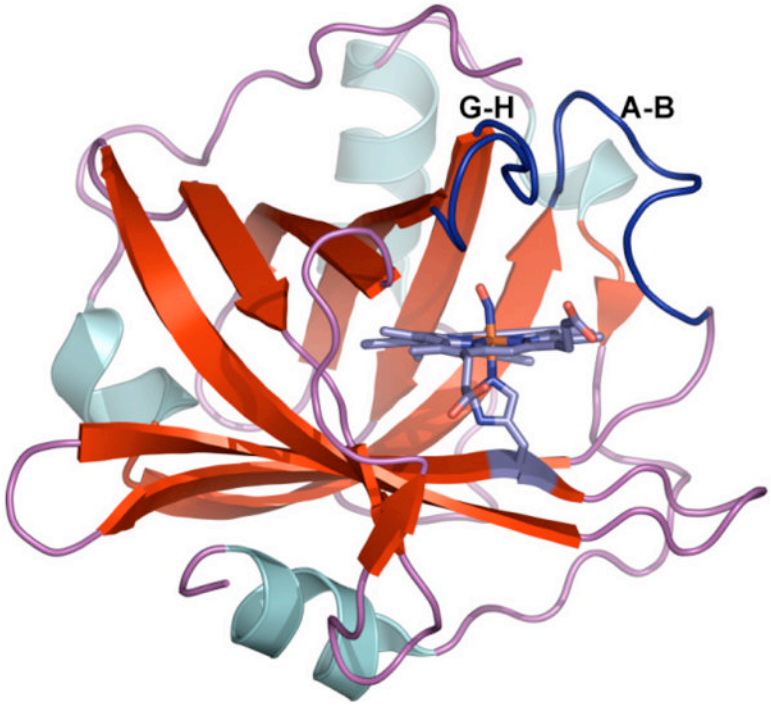

Figure 1.
Cartoon showing the NP4-NO protein at pH 5.6 (PDB ID: 1X8O). The positions of the loops A-B and G-H are highlighted in dark blue.

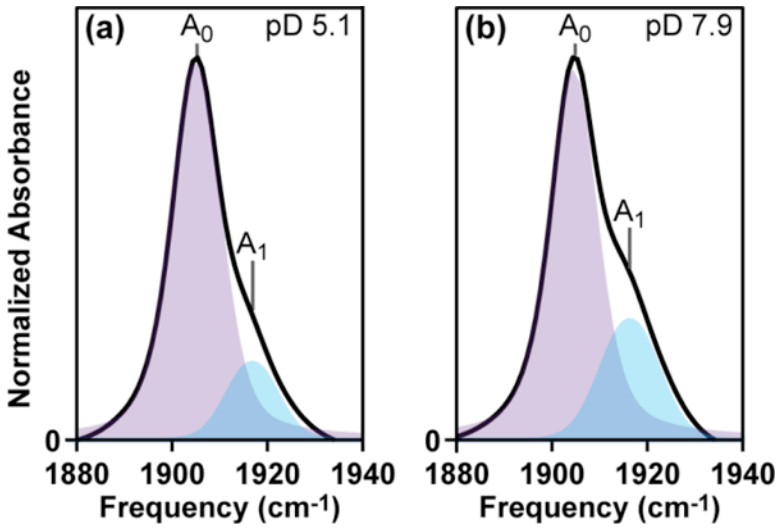

Figure 2.
pH-dependent FTIR spectra of NP4-NO. The shaded areas represent the fits of the two peaks using a Voigt lineshape.

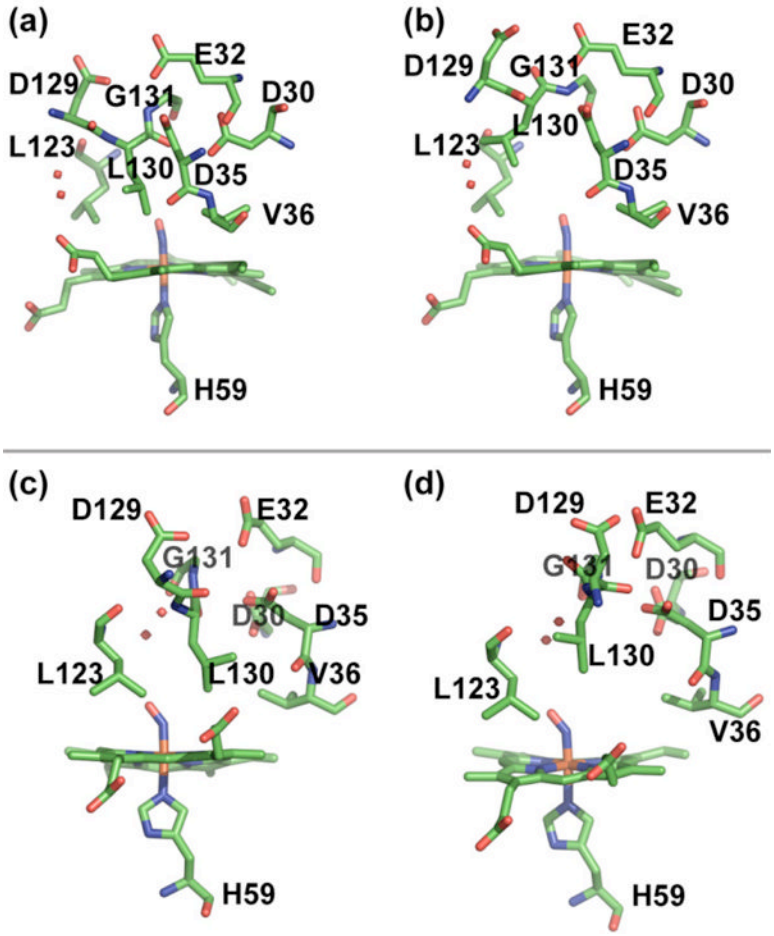

Figure 3.
Multiple conformers of NP4-NO determined by X-ray crystallography. The top panel shows the closed (3a) and open (3b) conformers at pH 5.6 (PDB ID 1X8O). The bottom panel shows the closed (3c) and open (3d) conformers at pH 7.5 (PDB ID 1X8N).

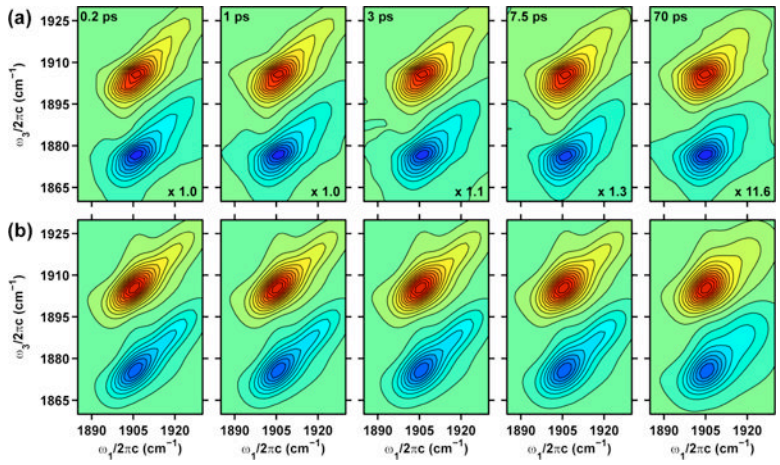

Figure 4.

(a) Experimental 2D IR spectra of the ν_{NO} in NP4-NO at pD 5.1. (b) Best fits to the experimental 2D IR spectra. Contour levels are drawn at 5% intervals. The τ_2 values and the normalization factors for each 2D plot are given in the top left and bottom right corners, respectively.

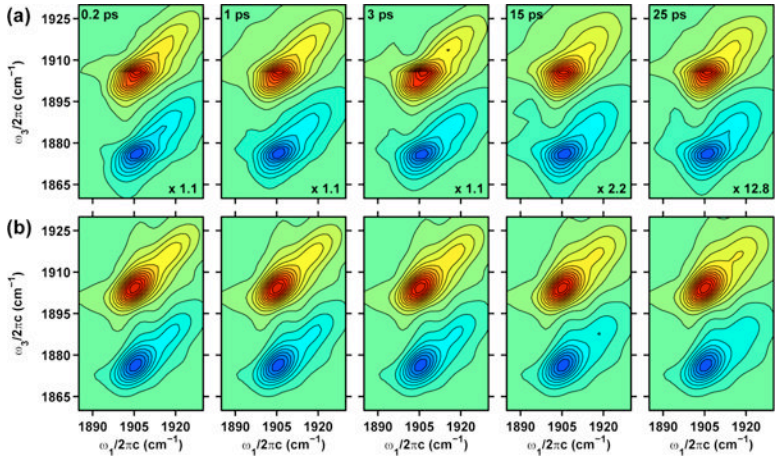

Figure 5.

(a) Experimental 2D IR spectra of the ν_{NO} in NP4-NO at pD 7.9. (b) Best fits to the experimental 2D IR spectra. Contour levels are drawn at 5% intervals. The τ_2 values and the normalization factors for each 2D plot are given in the top left and bottom right corners, respectively.

Table 1

Spectral characteristics of the ν_{NO} region in NP4-NO. The error bars correspond to a 95% confidence interval.

Peak	Sample pD	ν_{NO} (cm^{-1})	$\Delta\nu_{FWHM}$ (cm^{-1})
A_0	5.1	1904.9±0.2	11.7±0.4
A_1	5.1	1917±1	14±2
A_0	7.9	1904.3±0.2	12.1±0.4
A_1	7.9	1916±1	12±1

Table 2

Best fit parameters of the FFCF for the ν_{NO} in NP4-NO extracted from fitting the 2D IR data.

	Δ_1 (ps^{-1})	τ_{c1} (ps)	Δ_2 (ps^{-1})	τ_{c2} (ps)	T_2^* (ps)	Δ_{12} (cm^{-1})
pD 5.1						
A_0	0.55±0.04	3.0±0.1	0.57±0.05	∞	7±2	30±2
A_1	0.40±0.06	0.9±0.6	1.4±0.1	130±15	7±2	29±2
pD 7.9						
A_0	0.3±0.1	1.4±0.2	0.36±0.04	∞	7±2	30±2
A_1	0.57±0.07	0.8±0.2	1.2±0.1	70±15	7±2	29±2

J Phys Chem B. Author manuscript; available in PMC 2014 December 12.